

Chain desorption from a semidilute polymer brush: A Monte Carlo simulation

J. Wittmer

Institut Charles Sadron (C.N.R.S.-U.L.P.), F-67083 Strasbourg, France and Institut für Physik, Johannes Gutenberg-Universität Mainz, D-55099 Mainz, Germany

A. Johner and J. F. Joanny

Institut Charles Sadron (C.N.R.S.-U.L.P.), F-67083 Strasbourg, France

K. Binder

Institut für Physik, Johannes Gutenberg-Universität Mainz, D-55099 Mainz, Germany

(Received 16 February; accepted 28 April 1994)

We discuss the dynamic properties of a semidilute grafted polymer layer exposed to pure solvent. When the grafting energy of the head groups of the chains is finite, the chains desorb and are expelled from the layer. We combine Monte Carlo simulations using the bond fluctuation model to self-consistent mean field calculations and a scaling analysis. Chain desorption can be seen as a two step process. For strongly grafted polymers the limiting step is the desorption of the head group. The chain is then expelled by the osmotic pressure gradient. A chain cut off the wall is expelled at a constant velocity of its center of mass. The velocity decreases as the inverse of the molecular weight and increases with the grafting density. In the early stages of the expulsion the tension of the monomers close to the wall relaxes and the chain retracts. The retraction is independent of the molecular weight. Our most important result is that the desorption of the head group is a local process with a characteristic time independent of molecular weight. The desorption time increases exponentially with the grafting energy, it decreases as a power law of the grafting density. The exponent is close to 2 but the precise value is difficult to extract from the simulation.

I. INTRODUCTION

An efficient way to prevent the flocculation of colloidal particles in solution¹ is to coat them with a polymer layer. In this context, not only the static properties of the polymer layers are of importance but also their relaxation towards equilibrium and their exchange with the bulk solution. In this paper, we consider the coating of flat surfaces (large colloidal particles) by grafted polymer layers.² A grafted polymer layer is formed by chains with a functionalized head group that adsorbs onto a wall. When the grafting density is small, the different chains do not overlap, this is often referred to as the mushroom regime. When the grafting density is larger than the overlap value $\sigma_g^* \cong 1/R^2$ (where R is the radius of gyration of an isolated swollen chain in the bulk solution), the chains stretch from the surface and form a semidilute polymer brush.³

The equilibrium properties of polymer brushes were first described by Alexander and de Gennes using scaling arguments or *blob* pictures.⁴ The brush height h and the chain chemical potential μ are proportional to the molecular weight N and increase with the grafting density σ_g .

More recently Semenov⁵ has introduced a self-consistent field theory (SCF) which allows an explicit calculation of the monomer distribution. Zhulina *et al.* and Milner, Witten, and Cates⁶ have carried out detailed calculations for a semidilute brush in the strong stretching limit (high grafting density) showing that the monomer concentration profile is parabolic at the mean field level. The theory has also been extended to take into account the local swelling of the chains in a good solvent. The layer locally has the structure of a semidilute polymer solution, and the concentration fluctuations can be

described by a blob model. The correlation length (blob size) ξ increases towards the edge of the brush. At the brush edge, in the last correlation volume, the layer behaves as a dilute solution.

A density profile decreasing from the grafting surface was first observed for polymer brushes in a numerical study of the self-consistent field equations by Hirz.⁷ Since then both Monte Carlo and molecular dynamics simulations have confirmed the essential features of the SCF theory.⁸ To our knowledge however, no attempt was ever made to compare the simulation results to local excluded volume scaling laws for a brush in a good solvent.

In the last years, there has been an increasing interest in the dynamical properties of grafted polymer layers. Both theoretical models⁹ and simulations^{10,11} show a relaxation time of the chain ends distribution proportional to N^3 . More recently the full time-dependent monomer-monomer correlation function has been computed in a simulation by Chakrabarti and Marko,¹² confirming this scaling behavior.

The *formation* of a grafted layer from a solution of end functionalized polymers has been investigated by several groups.¹³ The experimental results of Tassin *et al.*, followed by others, have shown that the building up of the layer is a very slow process. This slow adsorption has been explained by the high energy barrier created by already grafted chains.¹⁴ Due to the slowness of this build-up of grafted layers, simulations¹⁵ are restricted to extremely short chains and hence cannot check the theoretical results in detail.

In this article, we focus on the *desorption* of initially grafted chains from the grafting surface and on the subsequent *expulsion* of those chains out of the semidilute brush.

Scaling arguments are compared with results obtained by Monte Carlo simulations extending the results of Lai.^{11,15}

We first describe the dynamics of a single chain cut off from the wall and driven out of the brush by the osmotic pressure gradient. In the early stages, the chain is far from equilibrium, it is anisotropically stretched in the direction perpendicular to the wall. The tension along the contour must then be relaxed while the center of mass is driven out.

We then consider the *washing* of a polymer brush where the chain heads have a finite grafting energy (e.g., $10 kT$).¹⁶ We discuss chain desorption when the layer is put in contact with a very dilute bulk solution. Experimentally this may be achieved by improving the solubility of the functionalized group that tethers the chain or by replacing the bulk solution by pure solvent. Our results might also be relevant for the interpretation of experiments on exchange of long chains with short ones in a polymer brush.¹⁷

The paper is organized as follows: In Sec. II we describe the simulation algorithm and the range of chosen parameters. In Sec. III we give a refined static study of a brush in a good solvent, which is needed in the exploitation of the dynamical simulations. The expulsion of single chains is described and compared with Monte Carlo results in Sec. IV. In Sec. V we show that the brush desorption rate at finite grafting energy is independent of the molecular mass. The consequences for adsorption and desorption processes are discussed in Sec. VI.

II. THE SIMULATION: TECHNICAL DETAILS AND RANGE OF PARAMETERS

The bond fluctuation model used in our simulation is a lattice Monte Carlo algorithm for macromolecular chains which is believed to reproduce Rouse dynamics correctly.¹⁸ It is described in detail elsewhere.¹⁹ Every “effective monomer” is represented by a cube of 8 lattice sites on a cubic lattice. To insure self-avoidance multiple occupation of lattice sites is forbidden. The bond vectors are allowed to vary between $2a$ and $\sqrt{10}a$ (a is the lattice spacing) imposing thus automatically chain connectivity; also nonergodicity of the algorithm (only a small fraction of “locked-in” configurations of the chains cannot be reached by the simulation) is not a problem in practical applications. The 108 allowed bond vectors connecting two consecutive monomers along a chain are obtainable from the set of coordinates (in units of the lattice spacing a) $\{(2,0,0), (2,1,0), (2,1,1), (2,2,1), (3,0,0), (3,1,0)\}$ by the symmetry operations of the cubic lattice.

The simulation box ($L_x = L_y = 30a, L_z = 150a$) is periodic in the x - and y -directions with impenetrable walls at $z=1$ and at $z=L_z$. The monodisperse chains are grafted on the $z=1$ plane where the grafted head groups move freely. The second hard wall at $z=L_z$ is so far away from the brush that its effect on the physical properties of the brush is quite negligible. Our results are sampled generally over 250 different brushes, except in Sec. V where only 50 brushes have been used.

The Monte Carlo procedure starts by choosing a monomer at random and trying to move it one lattice spacing in one of the randomly selected directions. The move is accepted only if (i) self-avoidance is satisfied; (ii) the new bonds still belong to the allowed set of bonds; and (iii)

$0 < z < L_z$. Following Lai¹⁵ we model the adsorption-desorption of end-functionalized chains onto the grafting plane in Sec. V by introducing an energy E_g gained when the head monomer is attached to the wall. A move where an end group is removed from the grafting wall is accepted if (iv) the Boltzmann factor $\exp(-E_g/kT)$ is larger than a random number uniformly distributed between 0 and 1.

Simulation results of monodisperse polymer chains of $N=20, 30, 40, 50, 100$ monomers are presented. (Chains with $N=10$ monomers were also studied but show strong finite size effects and are omitted.) The investigation of the crossover from Rouse to reptation dynamics for isotropic melts^{18,20} shows that for chains with up to 100 monomers Rouse scaling laws²¹ are observed. Dilute polymer chains in a good solvent have a diffusion constant D_0 inversely proportional to their molecular weight $ND_0 \approx 0.033 a^2/\text{MCS}$. Time is measured in attempted Monte Carlo steps per monomer (MCS). The Rouse relaxation time for the conformation of a single chain is given by $\tau_r^* \approx 5N^{1+2\nu}$ MCS (see Ref. 18 where the longest relaxation time is called τ_3). This time is roughly equal to the time taken by a chain to diffuse over a distance equal to its radius of gyration R , $R^2/6D_0 \approx 5.5N^{1+2\nu}$, where $R \approx 1.05aN^\nu$.

In the following, we define the overlap volume fraction as

$$\phi^* = 8 \frac{Na^3}{\frac{4\pi}{3} R^3} = 1.65N^{1-3\nu} \quad (2.1)$$

(the factor 8 is introduced because in the bond-fluctuation model each monomer occupies 8 lattice sites). When ever this is possible, the results are presented in scaled variables where the natural units R , ϕ^* , and τ_r^* are used. This leads to universal plots that can be compared to experiments with no adjustable prefactors. For example, ϕ/ϕ^* is the ratio of the molecular mass over the mass of polymer in a volume of radius R . The chemical potential per chain in a semidilute solution is calculated by Müller *et al.*²² as $3.4N\phi^{1/(3\nu-1)}$. Thus,

$$\mu_{\text{chain}} = 6.55(\phi/\phi^*)^{1/(3\nu-1)}. \quad (2.2)$$

Mushrooms and brushes with $M=1, 10, 20, \dots, 150$ chains on the surface have been simulated, corresponding to surface coverages of $\sigma=0.0044$ to 0.666 where

$$\sigma = 4\sigma_g a^2 = 4M/L_x L_y = (2a/d)^2. \quad (2.3)$$

The highest values (larger than 0.22) correspond already to brushes at polymer melt densities (e.g., $\sigma=0.6667$ corresponds to a average volume fraction of 0.54), since in the bond fluctuation model configurations with a volume fraction larger than 0.4 should be considered as melts.¹⁸ In the study of chain expulsion (Secs. IV and V) we use only surface fractions up to $\sigma=0.2222$.

Exponentially long relaxation times are expected²³ in polymer brushes when the dynamics is dominated by entanglements between different chains. However, Chakrabarti and Marko¹² have shown that Rouse-type dynamics (with screened hydrodynamic interaction) is observed in polymer brushes up to fairly high grafting densities. A significant

slowing down due to entanglements shows up only at the highest simulated densities (more than 20 blobs per chain). If not especially indicated, our simulated chains only have 5–15 blobs and we can thus ignore entanglements. Note that this seems to be the relevant experimental range.

The average bond length l and the acceptance rate A of attempted monomer moves are checked to be independent of N and to decrease both only slightly with the average monomer concentration $\langle\phi\rangle = 8N\sigma_g a^3/h \approx 3.3(\sigma_g a^2)^{2/3}$ [see Eq. (3.2b)]. The bond length is slightly larger than the bond length in an isotropic solution of the same average density.¹⁸ In the range of grafting densities studied both A and l can be considered as independent of the grafting density σ_g ($l \approx 2.69a$, $A \approx 0.25$).

Due to cage effects, the local monomer mobility m decreases much faster with increasing volume fraction than the acceptance rate. The mobility is the product of the square of the statistical segment length times the Rouse rate w setting the microscopic time scale for the diffusive processes. To compare simulation results with the Rouse model where the mobility is density independent, we rescale the times by the mobility. Using the data obtained in Ref. 18 the ratio of the mobility to the mobility $m^* \approx 0.0953$ at vanishing concentration ϕ is given by

$$\frac{m}{m^*} \approx 1 - 0.3467\phi - 6.8917\phi^2 + 8.6421\phi^3. \quad (2.4)$$

In the simulations of the expulsion process of Sec. IV we rescale the times by a mobility corresponding to the average monomer concentration $\langle\phi\rangle$ in the brush. The mobility ratio as a function of the grafting density is obtained by fitting the data of our simulations

$$\frac{m}{m^*} \approx 1 - 1.549\sigma - 0.824\sigma^2 + 1.979\sigma^3. \quad (2.4a)$$

As explained in Sec. V, for the desorption process at finite energy, the mobility is governed by the wall density $\phi(0)$. This leads to a much more important effect since $\phi(0) \approx 3/2\langle\phi\rangle$,

$$\frac{m}{m^*} \approx 1 - 3.506\sigma - 3.329\sigma^2. \quad (2.4b)$$

III. STATIC PROPERTIES OF POLYMER BRUSHES

The understanding of the desorption kinetics requires a detailed description of the equilibrium properties of the grafted polymer layer (Fig. 1). The static properties of polymer brushes have already been studied extensively, in this section we give a short reminder of the scaling properties and show some data obtained from our Monte Carlo simulations.

The characteristic length scale for noninteracting chains grafted on a planar surface (so-called mushrooms) in a good solvent is the Flory radius R . As the grafting density σ_g exceeds the overlap density $1/R^2$, the chains are strongly stretched and form a semidilute polymer brush. The brush height h scales as $h/R \approx (\sigma_g R^2)^\alpha$. Following de Gennes we require $h \sim N$ and obtain

$$\alpha = 1/2(1/\nu - 1) \approx 1/3. \quad (3.1)$$

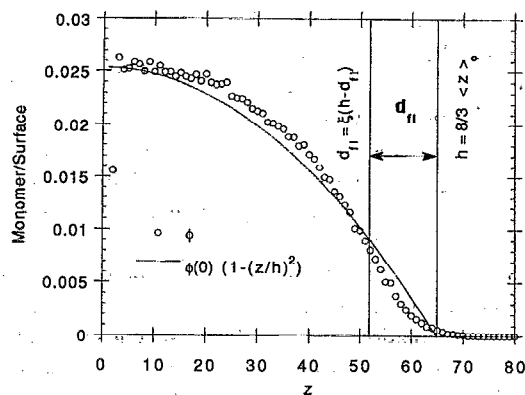
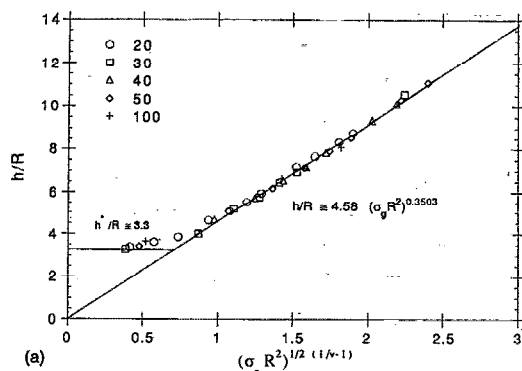
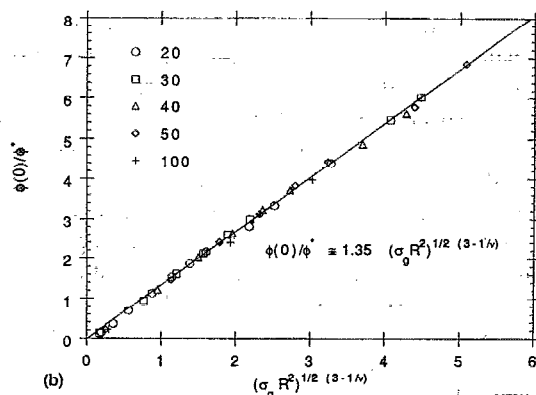


FIG. 1. The measured brush density profile for $(N, M) = (50, 20)$ compared with the parabolic density $\phi(0)[1 - (z/h)^2]$ using the measured brush height $h = 8/3\langle z \rangle \phi$. The fluctuations around the edge are described by the size of the last blob d_{II} defined by imposing $d_{II} = \xi(h - d_{II})$, where $\xi(z)$ is the screening length at distance z . In this example we have $h \approx 64.8a$, $d_{II} \approx 12.4a$.



(a)



(b)

FIG. 2. (a) The brush height $h = 8/3\langle z \rangle \phi$ compared with the Flory radius as a function of $(\sigma_g R^2)^{1/2(1/\nu-1)}$. (b) The volume fraction at the grafting plane is well described by $\phi(0)/\phi^* \approx 1.35(\sigma_g R^2)^{(3-1/\nu)/2}$. For surface fraction $\sigma = 0.222$ a volume fraction $\phi(0) \approx 0.4$ is obtained.

This scaling law is shown to be perfectly obeyed in Fig. 2(a). The brush height plotted there is the first moment of the brush density $h = 8/3 \langle z \rangle_\phi$, where the average is calculated with a weight proportional to the parabolic concentration profile predicted by the SCF mean field theory. We are dealing here with a good solvent brush and the density profile is not exactly parabolic, this only slightly affects the factor $8/3$ (Fig. 1). The agreement with the scaling law [Eq. (3.1)] remains quite good up to very large grafting densities even in the melt regime for our simulation model. At high densities, the two body interactions in the self-consistent field calculation must be replaced by a Flory free energy. In an athermal solvent, this free energy is dominated by the translational entropy of the solvent molecules and leads to an exponent $\alpha \approx 1/3$ over a very broad range of grafting densities if overstretching effects are ignored (nonlinear stretching of individual bonds).

A fit of the Monte Carlo results gives a brush height

$$h/R \approx 4.58(\sigma_g R^2)^{1/2(1/\nu-1)}. \quad (3.2a)$$

This result is in agreement with that of Lai and Binder¹¹ which is expressed in different units. The crossover from the mushroom regime to the semidilute brush occurs smoothly between $\sigma_g^* R^2 = 0.14$ and $\sigma_g^* R^2 = 0.53$, i.e., for an average distance between grafting points between $2.7R$ and $1.4R$.

The monomer volume fraction on the surface $\phi(0)$ is independent of the molecular mass and is proportional to $\sigma_g^{(3\nu-1)/2\nu} \approx \sigma_g^{2/3}$. In Fig. 2(b), $\phi(0)$ and σ_g are scaled by the corresponding overlap densities

$$\phi(0)/\phi^* \approx 1.35(\sigma_g R^2)^{(3\nu-1)/2\nu}. \quad (3.2b)$$

In the desorption problem, the energy scale is set by the chemical potential of one chain in the brush. As shown in Appendix A the simulation is in good agreement with simple scaling laws and the chain chemical potential varies as

$$\begin{aligned} \mu/kT &\approx 7.1[\phi(0)/\phi^*]^{1/(3\nu-1)} \\ &\approx 10.5(\sigma_g R^2)^{1/2\nu} \approx 0.26(h/R)^{1/(1-\nu)}. \end{aligned} \quad (3.3)$$

In the self-consistent mean field theory, the chain chemical potential varies as $\mu/kT = \pi^2/48 (h/R)^2$. This is very close to the simulation result with a slightly lower prefactor and a smaller exponent. When extrapolated to the mushroom regime the chemical potential is of the order of $1kT$ as expected, the strong stretching asymptotic limit is reached when the chemical potential exceeds $5kT$. The chemical potential is the same for all the possible chain conformations. In particular it is that of an unstretched chain with its non-grafted end close to the wall. It is thus interesting to compare the result of Eq. (3.3) to the chemical potential of a chain in a semidilute solution of concentration $\phi(0)$. We find a prefactor slightly larger than the one found for a semidilute solution in a similar simulation.¹⁸ Prefactors close to 7 are significantly higher than the universal amplitude for a semidilute solution given by Noda and des Cloizeaux²⁴ or Broseta et al.²⁵ that is closer to 3. However the conditions of the simulation are far from those of the universal limit of infinite mass, and vanishing concentration; the universal scaling could perhaps be recovered in a proper extrapolation.

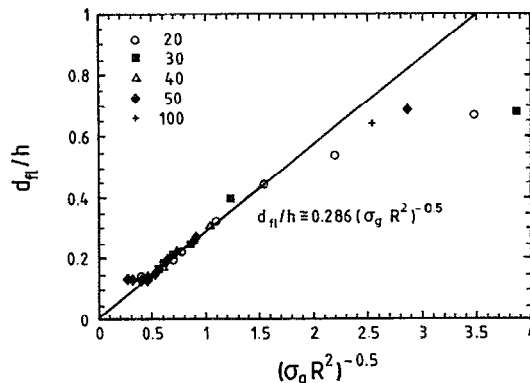


FIG. 3. The last blob size d_h reduced by the brush height as a function of $(\sigma_g R^2)^{-1/2}$. Decreasing the grafting density increases d_h and the depletion hole near the surface. To be consistent with the semidilute brush for grafting densities smaller than σ_g^* , d_h is taken to be the difference between $h^* = 8/3 \langle z \rangle_\phi$ and z_{\max} the position of maximal concentration. (For mushrooms we find $z_{\max} \approx R$, $h^* \approx 3.26R$.)

The simulated grafted layers are made of chains with a finite molecular weight and at a reasonable density the strong stretching assumption is not always valid (Fig. 1). In particular, at the outer edge of the layer there is a region where the tension of the chain vanishes and where concentration fluctuations become relevant. The size d_h of this region is small compared to the overall size of the layer for infinite chains but can reach a finite fraction of the overall layers for the chains considered here. The scaling form of the size d_h can be inferred by comparing the local correlation length in the brush to the distance to the edge of the brush. We define here the local correlation length as $\xi(z) = d[\phi(z)/\phi(0)]^{\nu/(1-3\nu)}$, where d is distance between grafting sites. We thus chose the numerical prefactor by imposing that on the grafting surface, the correlation length is equal to the distance between grafting sites. The size d_h is obtained by imposing that $\xi(h-d_h) = d_h$ and then expanding the density profile of the good solvent SCF version of a semidilute brush around the classical edge at $z=h$. Our simulations reported on Fig. 3 give the following law:

$$\frac{d_h}{h} \approx 0.286(\sigma_g R^2)^{-\beta} \quad \beta = 1/2. \quad (3.4)$$

This is in agreement with the theoretical scaling prediction.²⁶ Figure 3 also shows the crossovers from the brush regime to the mushroom regime and to the melt regime. While the crossover from the brush to the mushroom should be universal, the crossover to the melt (deviation from the straight line near the origin) is not universal, of course, and the details of the behavior there will depend somewhat on the details of the model. It is important to note that d_h/h can be as large as 10%–20% for brushes of physical interest and that in this portion of the layer, the chains only interact weakly and behave as in a dilute solution at the overlap concentration. The driving force that tends to expel

the chains from the brush vanishes there and expelled chains diffuse freely. This is important for the expulsion process studied in Sec. IV.

IV. EXPULSION OF A SINGLE CHAIN FROM THE BRUSH

We now discuss the kinetics of expulsion of one chain from the grafted layer. The brush is prepared at a given grafting density and is equilibrated. One of the chains randomly chosen is then cut off the wall and the subsequent motion of its monomers is studied.

In the mushroom regime, a given chain only has one characteristic time scale the Rouse time $\tau_r^* \equiv NR^2$. A grafted chain in the brush regime has two relaxation times, the relaxation time of the free end position τ_r and the, much faster, internal relaxation time of the chain conformation with a fixed end point τ_d .

The scaling laws for the end relaxation time τ_r and the internal relaxation time τ_d in the semidilute brush are obtained from the ansatz $\tau_r/\tau_r^* \sim (\sigma_g R^2)^\gamma$ and $\tau_d/\tau_r^* \sim (\sigma_g R^2)^\delta$. The equilibration of the chain ends distribution is governed by their diffusive motion over the grafted layer; the relaxation time is thus $\tau_r \sim h^2/D_0 \sim N^3$. The relaxation of the chain conformation with a fixed end point is governed by the usual Rouse dynamics and $\tau_d \sim N^2$. This gives

$$\gamma = 1/\nu - 1 \cong 2/3 \quad (4.1)$$

and

$$\delta = 1/2\nu - 1 \cong -1/6. \quad (4.2)$$

The same exponents can also be obtained from the Alexander-de Gennes blob analysis. These scaling laws are confirmed by numerical simulations; in Refs. 10 and 11, Eq. (4.1) was verified (the exponent of the grafting density strongly depends on the decrease of the mobility, discussed in Sec. II and could not be obtained).

When a single chain is cut off the wall, it is driven out of the layer by the osmotic pressure gradient. This process has been studied in the present simulations. The motions of the monomer initially grafted on the surface, of the central monomer and of the center of mass are plotted in Fig. 4.

The expulsion can be described within the framework of the Alexander blob model. The part of the chain which remains inside the brush is stretched while the monomers already expelled form a gaussian chain just outside the brush. At an intermediate time there are n monomers left in the brush, moving outwards with a velocity v . During the motion the viscous force is balanced by the driving force kT/d . Assuming Rouse dynamics, the total friction is $n\zeta v$ and $n\zeta v = kT/d$. The center of mass velocity is given by $Nv_{cm} = nv$, so that

$$v_{cm} \cong \frac{kT}{\zeta} \frac{1}{N} \sigma_g^{1/2}. \quad (4.3)$$

Over small length scales, the fluctuations of the center of mass positions are diffusive. The time necessary for the center of mass to diffuse over one blob is d^2/D_0 ; the drift velocity of the center of mass is the average velocity over one blob $v_{cm} \cong (d/(d^2/D_0))$, this gives back Eq. (4.3).

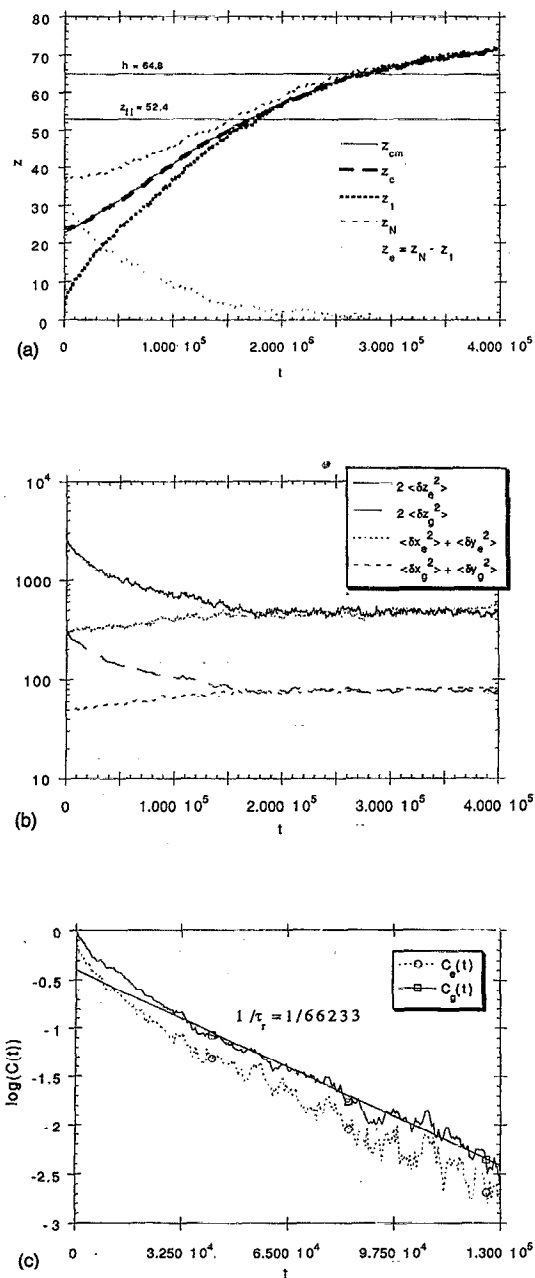


FIG. 4. (a) Desorption of one chain with $N=50$ out of a brush with surface fraction $\sigma=0.0889$. Due to the osmotic pressure gradient, the velocity of the center of mass and of the center monomer are constant as long as the chain is in the semidilute regime. The motion is getting diffusive in the dilute edge. Note that on the first monomer initially grafted on the wall is much faster than the center monomer due to the relaxation of the chain tension. It has traveled over several blobs before the cut-off-information has even reached the center monomer. (b) For the same simulation we compare $2\langle \delta x_{cm}^2 \rangle$ with $\langle \delta x_c^2 \rangle + \langle \delta y_c^2 \rangle$ and $2\langle \delta x_g^2 \rangle$ with $\langle \delta x_g^2 \rangle + \langle \delta y_g^2 \rangle$. (c) Plot of $\log[C_g(t)]$ and $\log[C_e(t)]$ against the time. $[C_e(t)]$ is defined similarly to $C_g(t)$.

As long as the center of mass has not reached the last blob of the brush the velocity is constant in good agreement with the simulation [Fig. 4(a)]. At the edge of the brush the motion becomes diffusive.

The velocity of the average center of mass position is a

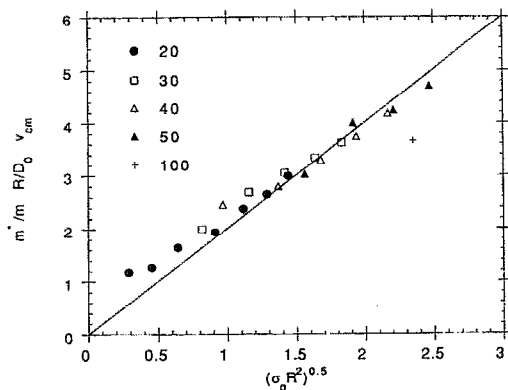


FIG. 5. Scaling plot of the reduced velocity $m/m^* v_{cm} R/D_0$ of the center of mass vs the square root of the reduced grafting density $\sigma_g R^2$. Data corresponding to different molecular weights N and different grafting densities collapse on a straight line with roughly a slope of 2.

well defined quantity and can be measured accurately. The velocity v_{cm} is plotted vs the grafting density σ_g in Fig. 5 where both v_{cm} and σ_g are divided by their values in the mushroom regime. According to Eq. (2.2) the times are rescaled with the mobility in a semidilute solution with a concentration equal to the average concentration in the brush. The mobility factor here affects only very weakly the results. We find $v_{cm} = 0.033 N^{-1} \sigma^{1/2} a / \text{MCS} \approx 2D_0/d$. Note that also for grafted chains the diffusion constant in the z -direction is $2D_0$.

The velocities for the only chain with $N=100$ (19 blobs) that we measured is slightly smaller than expected. This can mean the onset of reptation. Note that in the bulk for chains with $N=100$ the Rouse scaling gets worse, but this is still far from a pure reptation behavior (the large crossover regime is discussed in Ref. 18).

The expulsion time of the center of mass is

$$\tau_{cm} = \frac{h/2}{v_{cm}} \quad (4.4)$$

and is proportional to the relaxation time of the chain of blobs [Eq. (4.2)].

The scaling plot of the expulsion times τ_{cm} needed for the center of mass of a chain to leave the brush according to Eq. (4.4) is given in Fig. 6(a). The exponent $-1/6$ is too small to be seen in the simulation, but seems compatible with the horizontal line for the semidilute brush on the left side confirming the Rouse N^2 dependency of the time. There are two contributions to τ_{cm} , the time to cross the inner semidilute layer and the time to cross the dilute edge. For small grafting densities the diffusive contribution to τ_{cm} is dominant and gives rise to an increase of the expulsion time.

Just before the expulsion process, the grafted end point of the chain is not free and the chain tension at this point does not vanish. When the first monomer is cut off the surface it becomes free and its tension vanishes. The chain conformation must then relax and the chain retracts. This retraction is observed at short times ($t \ll \tau_d$) on the motion of the first monomer while the central monomer and the center of

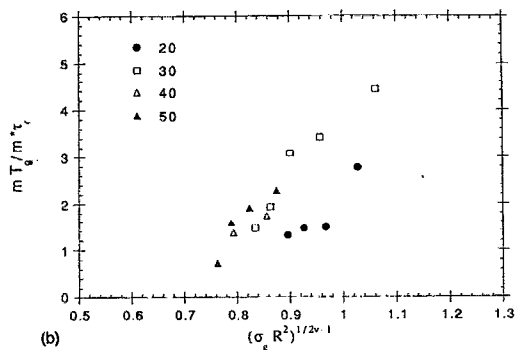
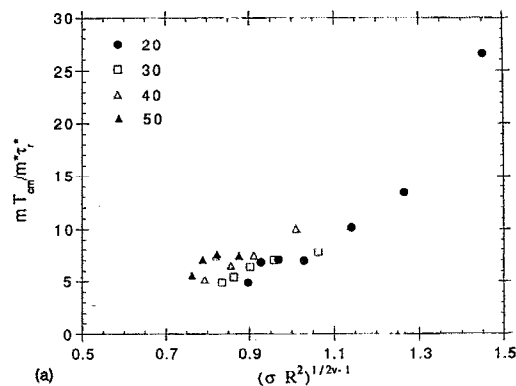


FIG. 6. (a) Scaling plot of the expulsion time rescaled with the mobility after Eq. (2.4), $m \tau_{cm} / \tau_r^* m^*$ against $(\sigma_g R^2)^{1/2\nu-1}$. (b) $m \tau_g / \tau_r^* m^*$ against $(\sigma_g R^2)^{1/2\nu-1}$.

mass still ignore that the chain is cut off the wall [Fig. 4(a)]. In this early time regime, the equation of motion of the first monomer is of the form $z_1/h \sim (t/\tau_d)^\alpha$. The motion is local and cannot depend on the molecular weight, this imposes $\alpha=1/2$. The position of the first monomer can then be written as $z_1/d \sim (t/\tau_0)^{1/2}$, where $\tau_0 \sim d^{2+1/\nu}$ is the Rouse relaxation time of the first blob in contact with the wall. This scaling law is consistent with the data of Fig. 4(a). It is also interesting to discuss the fluctuations around the average position of the first monomer. The fluctuations are governed by the standard Rouse dynamics and have an amplitude $\langle \delta z^2 \rangle \sim t^{2\nu/(1+2\nu)}$ [for a Gaussian chain, as shown in Appendix B, Eq. (B9), $\nu=1/2$ and $\langle \delta z^2 \rangle \sim t^{1/2}$]. As long as z_1 is larger than the size d of the blob, $z_1 \gg \delta z$ and the fluctuations are negligible. The head of the chain then has a negligible probability to come back to the wall. In the vicinity of the wall ($z_1 < d$) the fluctuations are dominant and $\delta z \gg z_1$. As long as it still is inside the first blob close to the wall, the first monomer has a high probability to bounce back on the grafting surface. This scaling analysis is in agreement with a detailed study of the Rouse equations of motion given in Appendix B.

The desorbed chain is initially stretched perpendicular to the surface and has an end-to-end distance $\langle \delta z_e^2 \rangle$ or a radius of gyration $\langle \delta z_g^2 \rangle$ proportional to N^2 . In a good solvent, the statistics lateral to the surface is not fully decoupled from the stretching in the z -direction resulting in a small but notice-

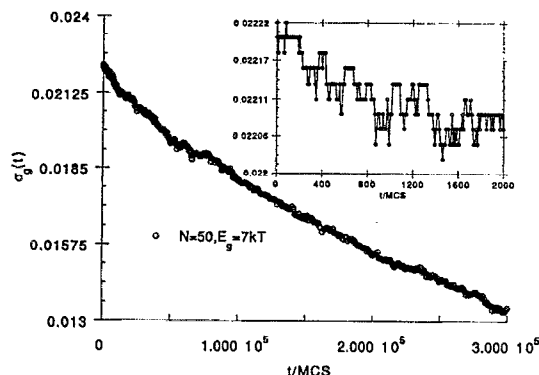


FIG. 7. Linear variation with time of the grafting density at short times for $N=50$, $M=20$, $E_g=10kT$ averaged over 50 configurations. The desorption rate here is $\Delta\sigma/\sigma\Delta t = -2.77 \cdot 10^{-3} \exp[-E_g/kT]$.

able decrease of $\langle \delta x_g^2 \rangle + \langle \delta y_g^2 \rangle$ and $\langle \delta x_g^2 \rangle + \langle \delta y_g^2 \rangle$ from their isotropic bulk values. A comparison of Figs. 4(a) and 4(b) shows that the chain is isotropic when it reaches the last dilute blob. The radius of gyration fluctuates less than the end-to-end distance and is now used to define the relaxation time τ_g of the chain anisotropy. We define the following correlation function to characterize the anisotropy:

$$C_g(t) = \frac{2\langle \delta z_g(t)^2 \rangle - \langle \delta x_g(t)^2 \rangle - \langle \delta y_g(t)^2 \rangle}{2\langle \delta z_g(0)^2 \rangle - \langle \delta x_g(0)^2 \rangle - \langle \delta y_g(0)^2 \rangle}. \quad (4.5)$$

The chain is isotropic for vanishing C_g and C_g is equal to 1 before the desorption. The longest relaxation time τ_g is obtained from the slope of the linear part in the log plot of Fig. 4(c). The scaling plot of the relaxation time τ_g given in Fig. 6(b) confirms the Rouse like N^2 scaling.

Note that the results of this section are not comparable directly to experiments where hydrodynamic interactions that we neglected here play a major role. A similar scaling analysis can however be carried out, the characteristic time being the Zimm time $\tau_z \sim R^3$. The constant velocity of expulsion is then $v_{cm} = kT/N\eta_s\sigma_g^{1/6}$, where η_s is the solvent viscosity.²⁷

V. WASHING OF A POLYMER BRUSH

In this section, we study the washing of polymer brushes. Grafted layers with grafting sites irreversibly adsorbed are prepared at equilibrium, the grafting energy is then suddenly decreased to a finite value E_g and the desorption process is observed. Up to now we have only considered athermal problems, temperature now enters via the finite interaction energy E_g between the wall and the first monomers penalizing the desorption of these monomers. We want to examine the desorption and ignore adsorption phenomena, we thus chose a large box ($L_z = 200a$). In the long time limit the translational entropy causes the desorption of all the chains (but a few mushrooms may remain).

At short times after the grafting energy has been set to a finite value the flux of chains from the grafting surface is constant as seen in Fig. 7 where the number of adsorbed chains per unit area is plotted. The hopping back and forth in

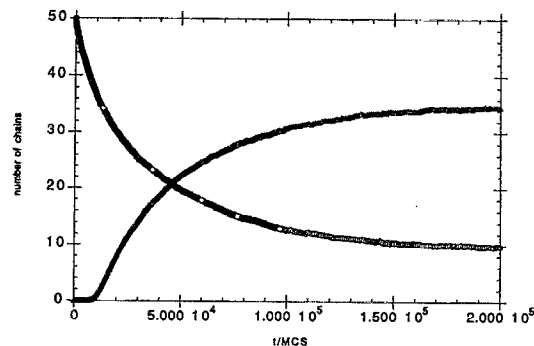


FIG. 8. The number of still grafted chains and the number of chains having reached the brush edge [$h(t) < R_{cmz}(t)$] as function of the time for a grafting energy $E_g=5kT$, chain length 20 and initial grafting density $\sigma_g=0.0556$.

the steep potential well creating the attraction is nicely seen. For a grafting energy $E_g=5kT$, a chain length 20 and an initial grafting density $\sigma_g=0.0556$, the desorption from the surface on a longer time scale is shown in Fig. 8. The number of chains having reached the brush edge has a similar variation with time; the curve is just shifted in time by the expulsion time from the brush as discussed in Sec. IV. Only in the latest stages of the washing does adsorption play a role due to the finite size of the simulation box. At the end of the process, only a few mushrooms remain grafted on the wall.

When the time is divided by $\exp(E_g/kT)$, the washing curves obtained for identical initial grafting densities collapse for grafting energies larger than $5kT$. For smaller values of the grafting energy, the desorption is faster (Fig. 9). The brush has then no time to relax during the desorption and cannot be considered as being in a quasiequilibrium state. Note that the initial configurations do not always correspond to a layer in equilibrium with a bulk solution at a concentration close to the overlap value. For instance, the configurations presented in Fig. 9, correspond to a chemical potential per chain of about $20kT$ from Eq. (3.3b).

In Fig. 10 we show that the desorption process does not depend on the molecular mass. The curve shown corresponds

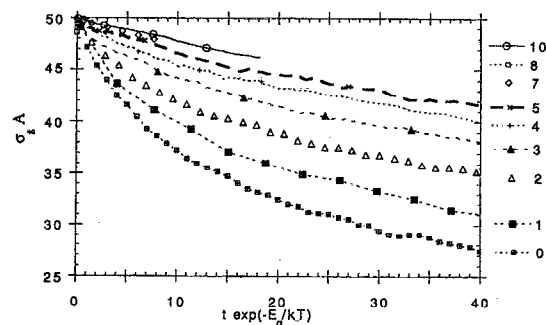


FIG. 9. Grafting density against the rescaled time $t \exp(-E_g/kT)$ for $(N, M) = (30, 50)$. For energies larger than 5 the desorption is slow enough and the curves are superimposed. The various symbols correspond to $E_g/kT = 0, 1, 2, 3, 4, 5, 7, 8$, and 10 (from down to top).

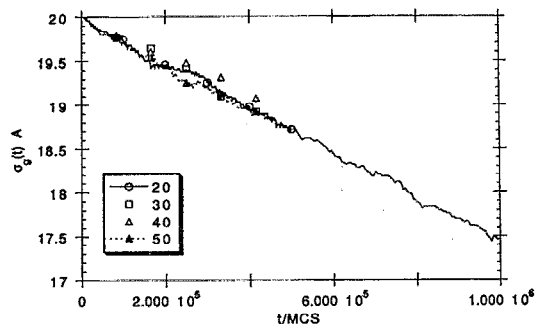


FIG. 10. Independence of the grafting density on molecular weight shown for an initial value of 0.0889 and an energy $10kT$.

to a grafting energy of $10kT$ and a grafting density σ_g of 0.0222 but this has been checked for several grafting densities (Fig. 10).

In order to desorb, a head group has to overcome an energy barrier of height E_g . Following the general framework of Kramers²⁸ rate theory, the prefactor $\exp(E_g/kT)$ is related to the escape by diffusion across the barrier about kT under its maximum. However the head group does not behave as a free particle. In the previous works done on this problem, it is generally assumed that the chain has to diffuse globally over a blob size in order that the head group overcomes the barrier, the effective friction is then proportional to the molecular mass. Therefrom a desorption flux proportional to $1/N$ is expected. In the simulation the molecular weight N varies over a sufficiently large range (20–100) to see a possible decrease of the desorption rate and no dependence on N is observed (Fig. 11). This suggests that the desorption of the head group is a local process, only the blob closest to the surface relaxes, the relevant friction is that of the blob and is independent of the chain length. This picture is also consistent with Sec. IV, where it is shown that after cutting the first monomer, the chain retracts and the motion of the first monomer is much faster than that of the central monomer of the chain.

The desorption time is of the form $T_- \cong \sigma_g^{-\beta} \times \exp(E_g/kT)$. The simulation does not allow for very accurate determination of the exponent β , but the value seems close to 2.

We have the following picture of the desorption process. The head group spends about $\exp(E_g/kT)$ steps hopping back and forth in the attractive well with a jump time τ_j , it then escapes the well and attempts to cross the first blob without being caught again by the well. To succeed in crossing the first blob and actually desorb the head group needs several attempts. A head group just leaving the well has probability P_{II} to diffuse across the first blob without coming back to the well, it thus needs $1/P_{II} - 1$ attempts to desorb. The desorption time is then $T_- = (1/P_{II} - 1) \tau_j \exp(E_g/kT)$.

As discussed in Sec. IV (and detailed in Appendix B) the motion of the first monomer in the blob close to the wall is dominated by diffusion rather than by the tension of the chain and due to the chain connectivity, the first monomer

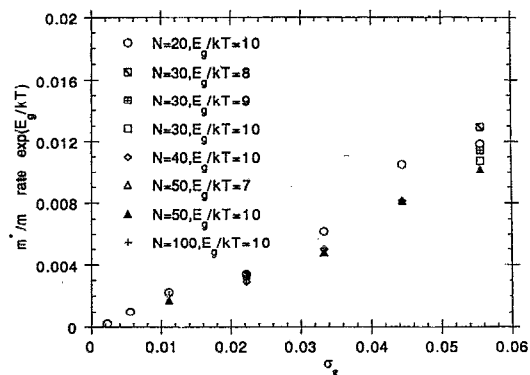


FIG. 11. The desorption rate $\Delta\sigma/\sigma\Delta t$ rescaled by $\exp(E_g/kT) m^*/m$ for different molecular weights against the grafting energy showing that the desorption is a local process at the grafting plane independent of the total chain properties.

has an anomalous diffusive motion, $\langle \delta z^2 \rangle \sim t^{2\nu/(1+2\nu)}$. This anomalous diffusion can be taken into account in a crude way by introducing a diffusion constant $D(\langle \delta z^2 \rangle)$. The scaling of the mean square displacement with time imposes $D \sim \langle \delta z^2 \rangle^{-1/2\nu}$.

The monomers of the chain are also subject to the impenetrable wall constraint, this leads to a strong decrease of the chain partition function when the chain end approaches the wall, and thus to a long range repulsion of the first monomer from the wall. It is shown in Appendix C that the long range potential $U(z)$ is given by $\exp(U/kT) \sim z^{-(1-\nu)/\nu}$.

The splitting probability at a distance d is calculated in Appendix C with these values of $D(z)$ and $U(z)$. The result is $1/P_{II} - 1 \cong (d/a)^2 \cong (\sigma a^2)^{-1}$. The splitting probability P_{II} that the first monomer reaches a distance z without hitting the wall when it is released close to the wall inside the brush has also been computed in the Monte Carlo simulation. Figure 12(a) shows that indeed the probability P_{II} is independent of N . It becomes constant when z is larger than the size d of the first blob and is proportional to the grafting density [Fig. 12(b)].

The time step for the long time hopping motion in the well is of the form $\tau_j \sim \zeta_\tau a^2$, where ζ_τ is the relevant friction. The simulation suggests that ζ_τ is the friction on the first blob $\zeta_\tau \sim \sigma^{-1/2\nu}$. With this conjecture

$$T_- \sim \sigma^{-(1+1/2\nu)} \exp(E_g/kT), \quad (5.1)$$

with $1+1/2\nu=11/6$. The value of ζ_τ is just a conjecture which gives good agreement with the simulations and for which we have no satisfactory derivation.

VI. CONCLUSION

We have presented a Monte Carlo simulation of a semi-dilute grafted polymer layer in a good solvent using the bond fluctuation model. The SCF theory extended to good solvents gives a reasonable description of the static properties of the brush; height, density of monomers at the wall, and chemical potential at thermodynamic equilibrium. The fluctuations around the classical trajectories of the chains in the brush are

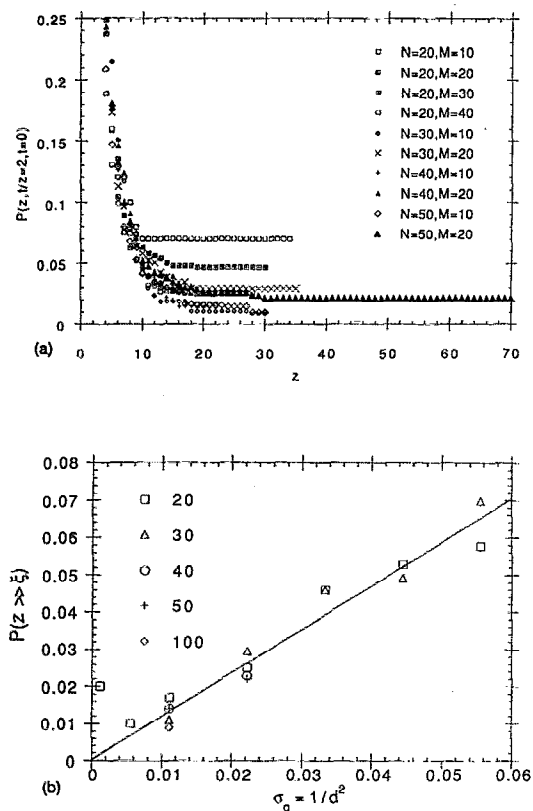


FIG. 12. (a) Splitting probability for several grafting densities and chain lengths showing the independency of molecular mass and the role of the first blob. (b) Plateau value of the splitting probability $P_{II}(z \geq l)$ against the grafting density $1/d^2$ for different molecular weights N .

important at the dilute edge. This dilute edge is small in the asymptotic limit of infinite chains but can be as large as a finite fraction of the total layer thickness for the finite chains used in most experiments. Our results for the static properties have been presented in the form of scaling relations involving only directly measurable physical quantities. The exponents and critical amplitudes compare rather well with the known theoretical predictions and the experimental values.

The main point of this paper is the study of the different dynamical processes involved in the washing experiment. We have identified two clearly different steps, the desorption of the head group and the expulsion of the center of mass from the brush.

The relaxation of the chain conformation and the expulsion of a single chain cut off the wall have been studied in Sec. IV. In the short time limit, the chain section close to the wall relaxes its tension. The first monomer rapidly moves over several blobs without any significant motion of the center of mass. The average distance of the first monomer from the wall increases as the square-root of time and the fluctuations around the average position are only important if the distance is smaller than a blob of size d (distance between grafting sites). Once the head group is beyond this blob the fluctuations in its position are small and the probability of readsorption by hitting back the wall is negligibly small.

The center of mass of the chain is expelled at a constant

velocity v_{cm} . Simultaneously the chain relaxes its anisotropy. At the dilute edge of the brush, the osmotic pressure gradient driving the expulsion vanishes and the motion of the center of mass becomes diffusive. The expulsion time scales as the Rouse relaxation time of a Gaussian chain of blobs and is proportional to N^2 . All the results can be understood by simple scaling arguments.

The washing of a brush with a finite grafting energy E_g exposed to pure solvent is considered in Sec. V. The characteristic time T_- for chain desorption increases exponentially with the grafting energy. The essential result is that T_- is independent of the molecular mass. This is consistent with the results of Sec. IV where we show that a head group which has left the first blob does not hit the wall again. The desorption is thus a local process. This result is in disagreement with the previous studies on polymer brush dynamics. The desorption time T_- decreases with the grafting density $T_- \sim \sigma_g^{-\beta} \exp(E_g/kT)$. The simulation does not give an accurate value for β , but β is close to 2. The exponent β depends both on the long range interaction between the head groups and the wall and on anomalous diffusion effects on short time scales. We were not able to provide a detailed analysis, but we suggest that T_- is proportional to the relaxation time of a blob and that $\beta=11/6$.

This result could also be important for the study of the kinetics of formation of grafted layer. Several existing theoretical studies treat the chain as a whole and consider only the motion of the center of mass. This work suggests that the crossing of the very high energy barrier due to the excluded volume could occur via fluctuations of the tension in the last blobs of the chain and thus be a much faster process.

ACKNOWLEDGMENT

J.W. thanks Bundesministerium für Forschung und Technologie (BMFT) for support under Grant No. 03M4040.

APPENDIX A: BRUSH SWOLLEN IN A GOOD SOLVENT

In the strong stretching approximation for strongly grafted brushes, the dominant contribution to the chemical potential per chain is proportional to the number of monomers and the entropy of the end points of the chains of order kT can be neglected. Fluctuations around the most probable conformation of the chain can be ignored and the configuration of each chain is obtained by minimization of the chemical potential functional $\mu(z)$ with respect to the position $z(n)$ of monomer n .

For a brush swollen in a good solvent we use the Widom-type free energy functional introduced by Milner et al.,^{6(b)}

$$\frac{\mu(z)}{kT} = \int_0^N dn \left[A(N) (\phi/\phi^*)^{(2\nu-1)/(3\nu-1)} \left(\frac{dz}{dn} \right)^2 + U(z) \right], \quad (A1)$$

$U(z) = B(N) (\phi/\phi^*)^{1/(3\nu-1)}$ is the work required to insert a monomer at a distance z from the wall. We have defined the prefactor $A(N)$ proportional to $\phi^{*(2\nu-1)/(3\nu-1)}$ and $B(N)$ to $\phi^{*1/(3\nu-1)} \cong 1/N$ with the overlap density $\phi^* = 3N/4\pi R^3$.

Due to the excluded volume correlations the elasticity term is not linear in z . The use of the coordinate Z defined by $dZ/dz = (\phi/\phi^*)^{1/2(2\nu-1)/(3\nu-1)}$ renormalizes the chain to a Gaussian string of swollen blobs.

In a monodisperse brush each configuration reaches the wall after N steps. This *equal-time requirement* imposes a parabolic potential in Z with a "spring constant" $k = 3\pi^2/8pa^2N^2$, where $l_p = pa$ is the persistence length of the chain so that

$$C(N)(Z_{\max}^2 - Z^2) = B(N)(\phi/\phi^*)^{1/(3\nu-1)} \quad (\text{A2})$$

with $C(N) = k\phi^{*(2\nu-1)/(3\nu-1)}$. In our model $C(N)R^2 = 0.623/N$. From Eq. (A2) the density profile can be implicitly obtained and Z_{\max} can then be eliminated from the normalization requirement

$$\sigma_g R^2 = 3/4 \pi \int_0^h dz/R \phi(z)/\phi^*.$$

The density at the wall is $\phi(0)/\phi^* = [C(N)Z_{\max}^2/B(N)]^{3\nu-1}$ or

$$\frac{\phi(0)}{\phi^*} = \left[\frac{C(N)R^2}{\alpha^2 B(N)} \right]^{(3\nu-1)/4\nu} (\sigma_g R^2)^{(3\nu-1)/2\nu} \quad (\text{A3})$$

with the numerical constant $\alpha = 3/4 \pi \int_0^1 du (1-u^2)^{2\nu-1/2} \cong 0.174$. From the definition of Z the brush height is given by

$$h/R = \int_0^{Z_{\max}} dZ/R [\phi(Z)/\phi^*]^{-1/2(2\nu-1)/(3\nu-1)}.$$

The elimination of Z_{\max} gives

$$\frac{h}{R} = \frac{\beta}{\alpha} \left[\frac{C(N)R^2}{\alpha^2 B(N)} \right]^{-(3\nu-1)/4\nu} (\sigma_g R^2)^{(1-\nu)/2\nu} \quad (\text{A4})$$

with the numerical constant $\beta = \int_0^1 du (1-u^2)^{-1/2(2\nu-1)} \cong 1.06$. Using the prefactors of Eq. (3.2) gives $B(N) = 7.1/N$.

The brush height is directly related to the density at the wall without any nonuniversal parameters

$$\frac{h}{R} = \frac{\beta}{\alpha} \frac{\sigma_g R^2}{\phi(0)/\phi^*} \quad (\text{A5})$$

in good agreement with the prefactors found in Eq. (3.2).

APPENDIX B: ROUSE ANALYSIS

When polymer chains are grafted on a solid surface, only Rouse modes that satisfy the constraints that the first monomer is on the surface $z(1,t) = 0$ and that the tension at the other end point vanishes $(\partial z/\partial n)(n=N) = 0$ are allowed. The amplitude of mode p varies as $z_p(n,t) = a_p \sin(\pi p n/2N) \exp(-t/\tau_p)$ where $\tau_p = 4N^2 a^2 \zeta / (p^2 - 1) \pi^2 kT$ is the relaxation time. The $p=1$ mode has an infinite relaxation time and gives the equilibrium conformation of the chains

$$z(n) = z \sin(\pi n/2N). \quad (\text{B1})$$

The equilibrium configuration of the layer is then specified by the density of chain free ends $g(z) = 3\sigma_g z/h^2 (1-z^2/h^2)^{1/2}$.

Once a chain is cut off the wall, the Rouse equation of motion for the monomers remains linear as long all its monomers stay in the parabolic mean field potential. We consider here only this short time limit. A chain in the layer non-grafted to the solid wall has its two ends free and the tension vanishes at both ends. The eigenmodes that satisfy this boundary condition are $z_p = a_p(t) \cos(np\pi/N)$. The dynamics of a chain with a configuration given by Eq. (B1) cut off the surface is calculated by projection onto the new eigenmodes,

$$z(n,t) = \sum_p a_p \cos(np\pi/N) \exp(-t/\tau_p), \quad (\text{B2})$$

where $\tau_p = \tau/(4p^2 - 1)$, with $\tau = 4N^2 a^2 \zeta / (\pi^2 kT)$. The amplitudes are

$$a_p = -\frac{4z}{\pi(4p^2 - 1)} \quad p \neq 0,$$

$$a_0 = \frac{2z}{\pi} \quad p = 0.$$

This gives the average position of the first monomer as a function of time

$$z(0,t) = \frac{2}{\pi} z \exp(t/\tau) \left[1 - 2 \sum_{p=1}^{\infty} \frac{1}{4p^2 - 1} \exp(-p^2 4t/\tau) \right]. \quad (\text{B3})$$

The sum can be calculated by Laplace transformation with respect to t/τ and is written as

$$z(0,t) = \frac{2}{\pi} z \exp(t/\tau) [1 - 2S(t/\tau)], \quad (\text{B4})$$

where $S(t/\tau)$ is the inverse Laplace transform of

$$S^*(s) = \frac{-1}{s+1} \frac{\pi}{4s^{1/2}} \coth\left(\frac{\pi s^{1/2}}{2}\right) + \frac{1}{2s}. \quad (\text{B5})$$

In the short time limit $t/\tau \ll 1$, the equation of motion of the first monomer is

$$z(0,t) = \frac{2z(t/\tau)^{1/2}}{\pi^{1/2}}. \quad (\text{B6})$$

This can now be averaged over the chain end distribution $g(z)$ at equilibrium to obtain

$$\langle z(0,t) \rangle_g = \frac{3}{16} \pi^{1/2} h (t/\tau_r^*)^{1/2}, \quad (\text{B6a})$$

where τ_r^* is the Rouse time of a single chain (Sec. II), this compares well with our simulation.

The position of the center of mass only depends on the first Rouse mode and varies as

$$z_G(t) = z_G(0) \exp(t/\tau). \quad (\text{B7})$$

This however supposes that all the monomers remain in the semidilute layer. Note that at short time this gives a constant velocity $z_G(t) = z_G(0)(1 + t/\tau)$ similar to the velocity v_{cm} obtained from the blob argument in the text.

The fluctuations around the average positions of the monomers are calculated by introducing the Langevin random forces in the Rouse equation. The calculation is very similar to the standard Rouse problem for an isolated free chain, the only effect of the parabolic potential is to change the value of the time τ . We obtain

$$\langle z^2 \rangle - \langle z \rangle^2 = \frac{kT\tau}{N\xi} [2 - \exp(2t/\tau) - 2 \exp(2t/\tau) S(2t/\tau)]. \quad (\text{B8})$$

In the short time limit $t/\tau \ll 1$ the fluctuation is thus

$$\langle z^2 \rangle - \langle z \rangle^2 = \frac{kT\tau}{N\xi} \pi^{1/2} (2t/\tau)^{1/2} \quad (\text{B9})$$

corresponding to the usual $t^{1/4}$ anomalous diffusion of a Rouse chain. At short time the fluctuation of the position is larger than its average value. The fluctuation becomes smaller than the average value when $\langle z \rangle$ is larger than $\sigma^{-1/3}$, i.e., than the mean-field blob size.

The essential result is that once the end group leaves the first blob, fluctuations are unlikely to bring it back in the adsorption well. This has been obtained here by neglecting the hard wall repulsion and hydrodynamic interactions but the result should qualitatively hold true when these are taken into account.

APPENDIX C: SPLITTING PROBABILITY

When a diffusing particle is released between two adsorbing planes I and II it has probability P_I to be caught by plane I and probability P_{II} to be caught by plane II. We calculate in this appendix the splitting probability P_{II}/P_I of a particle released at $z=a$ between the two adsorbing planes $z=0$ and $z=\xi$.

We start from the Fokker-Planck equation that the particle has probability density P to be in the interval $(z, z+dz)$ at time t for a particle diffusing in a potential $U(z)$,

$$\frac{\partial P}{\partial t} = \frac{\partial}{\partial z} \left[D \left(\frac{\partial P}{\partial z} + \frac{P}{kT} \frac{dU}{dz} \right) \right]. \quad (\text{C1})$$

The equation must be solved with adsorbing boundary conditions at $z=0$ and $z=\xi$; $P(0)=P(\xi)=0$. The probability P_{II} is the integral over time (from 0 to ∞) of the probability flux $J(z,t) = -D[(\partial P/\partial z) + (P/kT)(dU/dz)]$ across the $z=\xi$ plane. This is most conveniently obtained by Laplace transformation. We define the Laplace transform of $P(z,t)$ with respect to time as

$$P^*(z,s) = \int_0^\infty dt P(z,t) \exp(-st).$$

The Fokker-Planck equation gives then

$$sP^* - \delta(z-a) = \frac{\partial}{\partial z} \left[D \left(\frac{\partial P^*}{\partial z} + \frac{P^*}{kT} \frac{dU}{dz} \right) \right]. \quad (\text{C2})$$

The integral of the flux is its Laplace transform at $s=0$, we thus only need the solution of the Fokker-Planck equation at $s=0$. The probability P^* is expressed as two different stationary solutions vanishing on the adsorbing planes with a cusp singularity at $z=a$,

$$J_I^* = -D \left(\frac{\partial P^*}{\partial z} + \frac{P^*}{kT} \frac{dU}{dz} \right) \quad \text{for } 0 < z < a; \quad s=0, \\ J_{II}^* = -D \left(\frac{\partial P^*}{\partial z} + \frac{P^*}{kT} \frac{dU}{dz} \right) \quad \text{for } a < z < \xi; \quad s=0, \quad (\text{C3})$$

with $J_{II}^* - J_I^* = 1$ and $P^*(0,0) = P^*(\xi,0) = 0$.

The probability P_{II} that the particle reaches $z=\xi$ before $z=0$ is $J_{II}^*(0)$. The complementary probability is $P_I = -J_I^*(0)$ and the splitting probability reduces to $-J_{II}^*(0)/J_I^*(0)$.

We solve the above equations for $P^*(z,0)$ by matching the two stationary solutions (C3) and require continuity at $z=a$,

$$P_{II}/P_I = \frac{\int_0^a dz \exp(U/kT)/D(z)}{\int_a^\xi dz \exp(U/kT)/D(z)}. \quad (\text{C4})$$

This result is now applied to a Rouse chain. The Rouse dynamics of a polymer chain is approximately taken into account by considering each monomer as a free particle with an effective diffusion coefficient depending on the position $D(z) \sim z^{-1/\nu}$, where $z \equiv \langle \delta z^2 \rangle^{1/2}$.

The effective potential on the end point of the chain due to the hard wall constraint can be calculated by using a diffusion argument very similar to Eq. (C4). The self-avoiding walk is formally associated to an anomalous diffusion process where the effective time is the monomer index n . The correct scaling laws of the self avoiding walk are obtained from $d\langle \delta z^2 \rangle = D_W(z)dn$ with a diffusion constant $D_W(z) \sim z^{2-1/\nu}$. The fraction of walks starting at z and ending at about ξ without meeting the wall is proportional to $z^{(1-\nu)/\nu}$ after Eq. (C4) with $D(z) = D_W(z)$. The effective potential due to the impermeable wall constraint acting on the chain end is thus such that $\exp(U/kT) =$

$$P_I/P_{II} = \frac{\int_z^\xi dz' 1/D_W(z')}{\int_0^z dz' 1/D_W(z')} \\ \sim z^{-(1-\nu)/\nu} \quad \text{for } z \ll \xi.$$

Equation (C4) for the first monomer of the Rouse chain characterized by a diffusion constant $D(z)$ in this repulsive wall potential $U(z)$ gives $P_{II}/P_I \equiv (a/d)^2$, where the distance between grafting sites d is the size of the first blob [Fig. 12(b)].

¹ D. H. Napper, *Polymeric Stabilization of Colloidal Dispersion* (Academic, London, 1983).

² A. Halperin, M. Tirrell, and T. P. Lodge, *Adv. Polym. Sci.* **100**, 31 (1992).

³ P. Auroy, L. Auvray, and L. Leger, *Phys. Rev. Lett.* **66**, 719 (1991).

⁴ S. Alexander, *J. Phys. (Paris)* **38**, 983 (1977); P. G. de Gennes, *Macromolecules* **13**, 1069 (1980).

⁵ A. N. Semenov, *JETP Lett.* **61**, 733 (1985).

⁶ (a) E. B. Zhulina, V. A. Pryamitsyn, and O. V. Borisov, *Polym. Sci. USSR* **31**, 205, (1989); (b) S. T. Milner, T. A. Witten, and M. E. Cates, *Macro-*

- molecules **21**, 1610 (1988); (c) S. T. Milner, Z.-G. Wang, and T. A. Witten, *ibid.* **22**, 489 (1989).
- ⁷ S. J. Hirz, M.S. thesis, University of Minnesota, Minneapolis, Minnesota, 1988.
- ⁸ G. Grest and M. Murat, *Computer Simulations of Tethered Chains* (preprint, 1993).
- ⁹ A. Johner and J. F. Joanny, *J. Chem. Phys.* **96**, 6257 (1992). The $T \sim N^3$ behavior is also found by L. I. Klushin and A. M. Skvortzov, *Macromolecules* **24**, 1549 (1991).
- ¹⁰ M. Murat and G. S. Grest, *Phys. Rev. Lett.* **63**, 1074 (1989); *Macromolecules* **22**, 4054 (1989).
- ¹¹ P. Y. Lai and K. Binder, *J. Chem. Phys.* **95**, 9288 (1991); **97**, 586 (1992).
- ¹² J. F. Marko and A. Chakrabarti, *Phys. Rev. E* **48**, 2739 (1993).
- ¹³ J. F. Tassin, R. L. Siemens, W. T. Tang, G. Hadziioannou, J. D. Swallen, and B. A. Smith, *J. Phys. Chem.* **93**, 2106 (1989); H. Motschmann, M. Stamm, and C. Toprakcioglu, *Macromolecules* **24**, 3681 (1991).
- ¹⁴ C. Ligoure and L. Leibler, *J. Phys. (Paris)* **51**, 1313 (1990); A. Johner and J. F. Joanny, *Macromolecules* **23**, 5299 (1990); S. T. Milner, *ibid.* **25**, 5487 (1992).
- ¹⁵ P. Y. Lai, *J. Chem. Phys.* **98**, 669 (1993).
- ¹⁶ H. J. Taunton, C. Toprakcioglu, L. J. Fetters, and J. Klein, *Macromolecules* **23**, 571 (1990); J. Klein, D. Perahia, and S. Warburg, *Nature* **352**, 143 (1991); D. Perahia and J. Klein, *Phys. Rev. Lett.* **72**, 120 (1994).
- ¹⁷ E. Kumacheva, J. Klein, P. Pincus, and L. J. Fetters, *Macromolecules* **26**, 6477 (1993).
- ¹⁸ W. Paul, K. Binder, D. Heermann, and K. Kremer, *J. Phys. II* **1**, 37 (1991); *J. Chem. Phys.* **94**, 2294 (1991).
- ¹⁹ I. Carmesin and K. Kremer, *Macromolecules* **21**, 711 (1988); H. P. Deutsch and K. Binder, *J. Chem. Phys.* **94**, 2294 (1991).
- ²⁰ J. Wittmer, W. Paul, and K. Binder, *Macromolecules* **25**, 7211 (1992).
- ²¹ M. Doi and S. F. Edwards, *The Theory of Polymer Dynamics* (Clarendon, Oxford, 1986).
- ²² M. Müller and W. Paul, *J. Chem. Phys.* **100**, 719 (1994).
- ²³ S. P. Obukhov and M. Rubinstein, *Phys. Rev. Lett.* **17**, 1856 (1993). For the related case of star polymers, T. A. Witten, L. Leibler, and P. Pincus, *Macromolecules* **23**, 824 (1990).
- ²⁴ J. des Cloizeaux and I. Noda, *Macromolecules* **15**, 1505, (1982).
- ²⁵ D. Broseta, L. Leibler, A. Lapp, and C. Strazielle, *Europhys. Lett.* **2**, 733 (1986).
- ²⁶ A. Johner and J. F. Joanny, *J. Chem. Phys.* **98**, 1647 (1993).
- ²⁷ A. Halperin and S. Alexander, *Europhys. Lett.* **6**, 329 (1988); *Macromolecules* **22**, 2403 (1989).
- ²⁸ N. G. Van Kampen, *Stochastic Processes in Physics and Chemistry* (North-Holland, Amsterdam, 1981).